Flux Flow of Abrikosov-Josephson Vortices along Grain Boundaries in High-Temperature Superconductors

A. Gurevich,[1] M. S. Rzchowski,[1,2] G. Daniels,[1] S. Patnaik,[1] B. M. Hinaus,[3]
F. Carillo,[4] F. Tafuri,[4] and D. C. Larbalestier[1]

[1]*Applied Superconductivity Center, University of Wisconsin, Madison, Wisconsin*
[2]*Department of Physics, University of Wisconsin, Madison, Wisconsin*
[3]*Department of Physics, University of Wisconsin, Stevens Point, Wisconsin*
[4]*Universita di Napoli Federico II, Dipartamento di Scienze Fisiche, Italy*

(Received 27 July 2001; published 13 February 2002)

Low-angle grain boundaries (GBs) in superconductors exhibit intermediate Abrikosov vortices with Josephson cores, whose length l along GB is smaller than the London penetration depth, but larger than the coherence length. We found an exact solution for a periodic vortex structure moving along GBs in a magnetic field H and calculated the flux flow resistivity $R_F(H)$, and the nonlinear voltage-current characteristics. The predicted $R_F(H)$ dependence describes well our experimental data on 7° unirradiated and irradiated $YBa_2Cu_3O_7$ bicrystals, from which the core size $l(T)$, and the intrinsic depairing density $J_b(T)$ on nanoscales of a few GB dislocations were measured for the first time. The observed $J_b(T) = J_{b0}(1 - T/T_c)^2$ indicates a significant order parameter suppression on GB.

DOI: 10.1103/PhysRevLett.88.097001 PACS numbers: 74.20.De, 74.25.Ha, 74.60.–w

Mechanisms of current transport through grain boundaries (GBs) in high-temperature superconductors (HTS) have attracted much attention, because a GB is a convenient tool to probe the pairing symmetry of HTS by varying the misorientation angle ϑ between the neighboring crystallites [1,2]. As ϑ increases, the spacing between the GB dislocations decreases, becoming comparable to the coherence length $\xi(T)$ at the angle $\vartheta_0 \simeq 4°$–$6°$. The exponential decrease of the GB critical current density $J_b = J_0 \exp(-\vartheta/\vartheta_0)$ [2], makes GBs one of the principal factors limiting critical currents of HTS [3]. Atomic structure of GBs revealed by high-resolution electron microscopy have been used to determine local underdoped states of GB, defect-induced suppression of superconducting properties at the nanoscale and controlled increase of J_b by overdoping of GB [2,4]. Much progress has been made in understanding the microscopic factors controlling $J_b(\vartheta)$ at zero magnetic field, but the behavior of vortices on GBs is known to a much lesser extent.

The extreme sensitivity of $J_b(\vartheta)$ to the misorientation angle makes GB a unique tool to trace the fundamental transition between Abrikosov (A) and Josephson (J) vortices [5] in a magnetic field H above the lower critical field H_{c1}. For $\vartheta \ll \vartheta_0$, vortices on a GB are A vortices with normal cores pinned by GB dislocations [6]. For $\vartheta > \vartheta_0$, the maximum vortex current density circulating across the GB is limited to its *intrinsic* $J_b(\vartheta)$, much smaller than the bulk depairing current density J_d. Because vortex currents must cross the GB which can only sustain $J_b \ll J_d$, the normal core of an A vortex turns into a J core, whose length $l \simeq \xi J_d/J_b$ along the GB is greater than ξ, but smaller than the London penetration depth λ, if $J_b > J_d/\kappa$, where $\kappa = \lambda/\xi \simeq 10^2$ [5]. As ϑ increases, the core length $l(\vartheta) \simeq \xi J_d/J_b(\vartheta)$ increases, so the GB vortices evolve from A vortices for $\vartheta \ll \vartheta_0$ to mixed Abrikosov vortices with Josephson cores (AJ vortices) at $J_d/\kappa < J_b(\vartheta) < J_d$. The AJ vortices turn into J vortices at higher angles, $\vartheta > \vartheta_J \simeq \vartheta_0 \ln(\kappa J_0/J_d)$, for which $l(\vartheta)$ exceeds λ. For $\vartheta_0 = 5°$, $\kappa = 100$, and $J_0 = J_d$, the AJ vortices determine the in-field behavior of GBs in the crucial region $0 < \vartheta < \vartheta_J \simeq 23°$ of the exponential drop of $J_b(\vartheta)$ [in a film of thickness $d \ll \lambda$, the AJ region $\vartheta < \vartheta_J \simeq \vartheta_0 \ln(\lambda^2/d\xi)$ broadens even further].

The AJ structures have two length scales: the core size $l > \xi$ and the intervortex spacing $a = (\phi_0/B)^{1/2}$. The larger core of AJ vortices leads to their weaker pinning along a GB, which thus becomes a channel for motion of AJ vortices between pinned A vortices in the grains [5,7] (Fig. 1). The percolative motion of AJ vortices gives rise to a linear region in the V-I characteristic of HTS polycrystals [6,8–11]. However, no present experimental techniques can probe the cores of GB vortices, because the lack of the normal core makes AJ vortices "invisible" under STM, while neither the Lorentz microscopy nor magneto-optics have sufficient spatial resolution to distinguish A and AJ vortices. In this Letter, we report a combined theoretical and experimental analysis which enabled us to prove the existence of AJ vortices in 7° $YBa_2Cu_3O_7$ bicrystals and extract the core size $l(T)$, and the intrinsic J_b at the GB from transport measurements. The value of J_b turns out to be much higher than the GB global critical current density J_{gb}, which is limited by self-field and pinning effects [7,10–13]. The field region in which only a single AJ vortex chain moves along GB while A vortices remain pinned, can be considerably expanded by irradiation.

For $H \gg H_{c1}$, both l, and $a(B)$ are smaller than λ, thus the AJ vortices are described by a nonlocal equation for the phase difference $\theta(x,t)$ on a GB [5,7]:

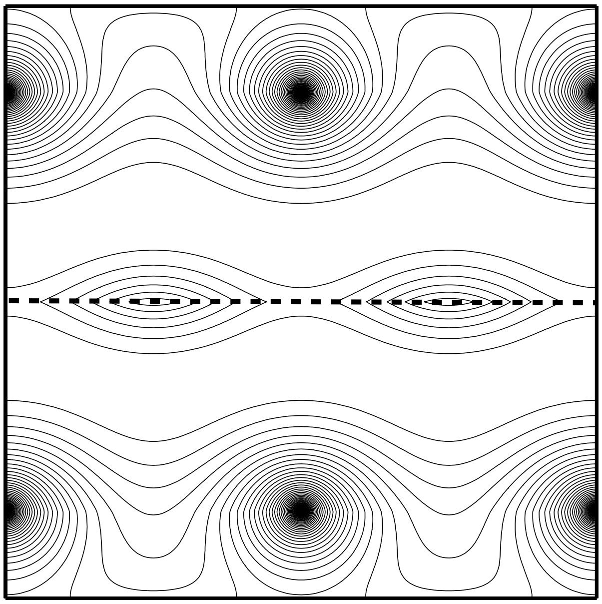

FIG. 1. Current streamlines around AJ vortices on a GB (dashed line) and the bulk A vortices in the grains, calculated from Eq. (5) for $l = 0.2a$.

$$\tau\dot{\theta} = \frac{l}{\pi}\int_{-\infty}^{\infty}\frac{\theta'(u)\,du}{u - x} - \sin\theta + \beta\,, \qquad (1)$$

$$l = c\phi_0/16\pi^2\lambda^2 J_b, \qquad \tau = \phi_0/2\pi cRJ_b\,, \qquad (2)$$

where the overdot and the prime denote differentiation with respect to the time t and the coordinate x along GB, R is the quasiparticle resistance of GB per unit area, ϕ_0 is the flux quantum, c is the speed of light, $\beta = J/J_b$, and $J(x)$ is the current density through GB induced by A vortices. Here $\beta = \beta_0 + \delta\beta(x)$ is a sum of the constant transport current β_0 and an oscillating component $\delta\beta(x)$ due to the discreteness of the A vortex lattice. The term $\delta\beta(x)$ gives rise to a critical current J_{gb} of the GB due to pinning of AJ vortices by A vortices in the grains [7]. Equations (1) and (2) are independent of the pairing symmetry (which only affects J_b) and are valid for both bulk samples and thin films in a perpendicular field.

We consider a rapidly moving AJ structure in the flux flow state, $\beta \gg \beta_c$, for which the pinning term $\delta\beta(x) \ll 1$ can be neglected. In this case Eq. (1) has the following *exact* solution that describes a stable periodic vortex structure moving with a constant velocity v:

$$\theta = \pi + \gamma + 2\tan^{-1}[M\tan k(x - vt)/2], \qquad (3)$$

$$s^2 = [\sqrt{(1 - \beta_0^2 + h)^2 + 4\beta_0^2 h} - 1 - h + \beta_0^2]/2h\,. \qquad (4)$$

Here $s = v/v_0$, $v_0 = l/\tau$, $\tan\gamma = -s$, $h = (kl)^2$, $M = [1 + 1/h(1 + s^2)]^{1/2} + [h(1 + s^2)]^{-1/2}$, $k = 2\pi/a$, and a is the period of the AJ structure. For $a/l \to \infty$, Eq. (3) describes a moving chain of single AJ vortices [5]. Generally, $a(H)$ is different from the period of the A lattice, but for $H \gg H_{c1}$, the spacing $a = (\phi_0/H)^{1/2}$ is fixed by the flux quantization condition. Equation (3) corresponds to the following field distribution $H(x,y)$ produced by AJ vortices in the region $|y| < \lambda$:

$$H = \frac{\phi_0}{2\pi\lambda^2}\,\mathrm{Re}\ln\sin[x - vt + i(|y| + y_0)]\,\frac{k}{2}\,, \qquad (5)$$

where $\sinh ky_0 = \sqrt{h(1 + s^2)}$. Equation (5) satisfies the Maxwell equation $\nabla^2 H = 0$ with the boundary condition $H' = (4\pi/c)[J_b\sin\theta - \hbar v\theta'/2eR - J]$ on GB, where $\theta(x,t)$ is given by Eq. (3). Figure 1 shows the current streamlines calculated from Eq. (5). For $y > 0$, these streamlines coincide with those of a chain of moving fictitious A vortices displaced by $y = -y_0$ away from GB.

The mean voltage V on a GB is determined by the Faraday law, $V = \phi_0 v/ca$, which yields

$$V = V_0[\sqrt{(1 - \beta_0^2 + h)^2 + 4\beta_0^2 h} - 1 - h + \beta_0^2]^{1/2}, \qquad (6)$$

where $V_0 = RJ_b/\sqrt{2}$. The V-J curve shown in Fig. 2 is similar to that obtained by molecular dynamic simulations of incommensurate vortex channels [14]. In our case the nonlinearity of $V(J)$ is due to the AJ core expansion as J increases [5]. For $J \ll J_b$, the V-J curve is linear, $V = R_F J$, where $R_F = R\sqrt{h/(1 + h)}$ is the flux flow resistivity due to the viscous motion of AJ vortices. If $H \gg H_{c1}$, then $h = (2\pi l/a)^2 = H/H_0$, and

$$R_F = \frac{R\sqrt{H}}{\sqrt{H + H_0}}\,, \qquad H_0 = \frac{\phi_0}{(2\pi l)^2}\,. \qquad (7)$$

At $H \ll H_0$, Eq. (7) describes $R_F(H)$ for AJ vortices, whose cores do not overlap. In this case $R_F(H)$ is reminiscent of the 1D Bardeen-Stephen formula, $R_{BS} \simeq R\sqrt{H/H_{c2}}$, except that in Eq. (7) the core structure is taken into account exactly. For $H > H_0 \simeq (J_b/J_d)^2 H_{c2} \ll H_{c2}$, the AJ cores overlap, and Eq. (7) describes a crossover to

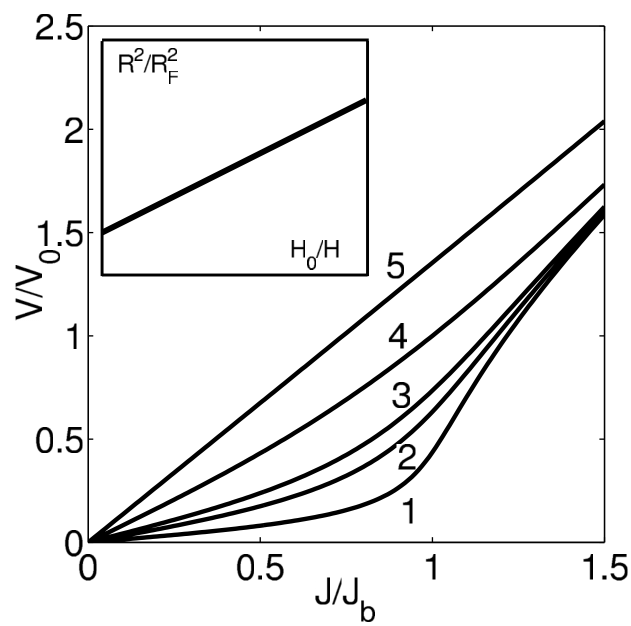

FIG. 2. The V-J curves calculated from Eq. (6) for different magnetic fields $h = H/H_0$: 0.01(1), 0.05(2), 0.1(3), 0.5(4), 10(5). The inset shows the field dependence of $R_F(H)$.

the quasiparticle resistance of GB. This regime has no analogs for A vortices, whose normal cores overlap only at H_{c2}. The simplicity of Eq. (7) enabled us to extract intrinsic GB properties from the measurements of $R_F(H)$.

We observed the AJ vortex behavior on 7° $YBa_2Cu_3O_7$, bicrystals with a sharp resistive transition $\Delta T < 0.4$ K at $T_c = 91$ K. Thin films of thickness 250 nm were grown on [001]-oriented $SrTiO_3$ bicrystals by pulsed laser deposition at 210 mTorr oxygen pressure and 810 °C, and then annealed in oxygen at 830 Torr and 520 °C for 30 min. One 7° bicrystal was irradiated with 1 GeV Pb ions at a fluence corresponding to 1 T. Bridges 25 μm wide were patterned by Ar ion beam etching on a cooled sample mount to produce a four-point measurement geometry, as described in Ref. [9]. The voltage probes were 100 μm apart, on either sides of the GB. V-I curves were measured in a gas-flow cryostat in fields $0 < H < 10$ T. The intragrain $J_c(77\text{ K})$ values were 0.1 and 0.27 MA/cm^2 for the unirradiated and irradiated samples, respectively.

For the unirradiated sample at 77 K, the V-I characteristics shown in Fig. 3 exhibit linear flux flow portions in a wide range of I above the depinning current $I_{gb}(H)$ which decreases with H [13]. For $I \gg I_{gb}$, the flux flow resistance $R_F(H) = dV/dI$ increases as $\sqrt{H}$ at low H, but levels off at higher H. Equation (7) describes the observed $R_F(H)$ very well, thus the vortex cores on this GB overlap at $H \sim H_0$, well below H_{c2}. Because the GB can sustain a finite supercurrent I_{gb} even for $H > H_0$, the GB vortices lack normal cores. The fit in Fig. 3 gives $R = 4.05$ mΩ and $H_0 = 0.14\text{ T} \ll H_{c2}$. Using Eq. (7), we obtain that $l = (\phi_0/H_0)^{1/2}/2\pi = 190$ Å at 77 K, thus vortices on this 7° GB are indeed AJ vortices with phase cores much greater than $\xi(T) = \xi_0/\sqrt{1 - T/T_c} \simeq 40$ Å but smaller than $\lambda = \lambda_0/\sqrt{1 - T/T_c} \simeq 4000$ Å for $\xi_0 \simeq 15$ Å, $\lambda_0 \simeq 1500$ Å, and $T_c = 91$ K.

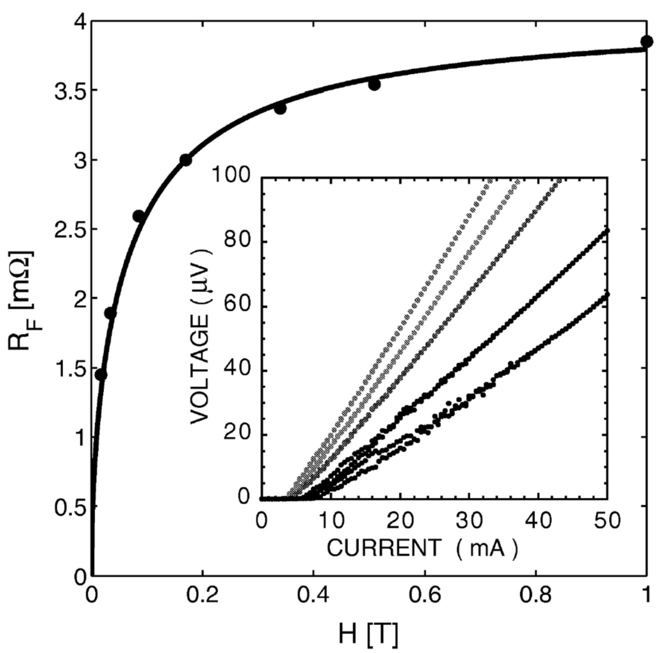

FIG. 3. $R_F(H)$ data extracted from the slopes of the $V(J, H)$ curves at 77 K for the unirradiated bicrystal. The solid curves are described by Eq. (7) with $R = 4.05$ mΩ and $H_0 = 0.14$ T. The inset shows V-J curves for 0.17, 0.51, 0.85, 1.7, and 3.4 kOe (from bottom to top, respectively).

$R_F(H)$ data for the irradiated bicrystal are shown in Fig. 4. The good agreement between Eq. (7) and the observed $R_F(H)$ enabled us to extract the temperature dependences of H_0 and R shown in Fig. 5. While $R(T)$ varies only weakly, the field $H_0(T)$ exhibits a parabolic dependence, $H_0(T) = H_0(0)(1 - T/T_c)^2$ with $H_0(0) \approx 42$ T. As follows from Eq. (7), the fact that $H_0(T) \propto (T_c - T)^2$ implies $l(T) \propto (T_c - T)^{-1}$, which, in turn indicates the SNS behavior of $J_b(T) \propto (T_c - T)^2$, if $\lambda(T) \propto (T_c - T)^{-1/2}$ in Eq. (2). From the data in Fig. 5, we can also obtain the intrinsic depairing current density J_b averaged over the Josephson core length l. To do so, we write Eq. (7) in the form $J_b = (3J_d/4)\sqrt{6\pi H_0/H_{c2}}$, which express J_b in terms of the measured parameters H_0, $H_{c2} = \phi_0/2\pi\xi^2$, and $J_d = c\phi_0/12\sqrt{3}\,\pi^2\lambda^2\xi$. For $H_{c2}(T) = H_{c2}'(T_c - T)$, this yields $J_b \simeq (3J_d/4)[6\pi H_0(0)/T_c H_{c2}']^{1/2}(1 - T/T_c)^{1/2}$, whence $J_b(85\text{ K}) \simeq 0.3J_d(85\text{ K})$ for $H_0(0) = 42$ T, and $H_{c2}' = 2T$/K. Likewise we get $J_b(77\text{ K}) \simeq 0.23J_d(77\text{ K})$ for the unirradiated sample, $[H_0(77\text{ K}) = 0.14\text{ T}]$. Therefore, our data indicate a significant suppression of the order parameter, even on the low-angle 7° GB, in agreement with the model of Ref. [15].

For the observed $H_0(T)$, the AJ core length $l(T) = [\phi_0/H_0(T)]^{1/2}/2\pi \simeq 11(1 - T/T_c)^{-1}$ [Å], exceeds the bulk coherence length $\xi(T) = \xi_0/\sqrt{1 - T/T_c}$ at $T_c - T \ll T_c$, but remains smaller than $\lambda(T)$, except very close to T_c. For instance, we obtain $l(80\text{ K}) \simeq 91$ Å, while $\xi(80\text{ K}) \simeq 43$ Å, and $\lambda(80\text{ K}) = 4300$ Å. The length $l(T)$ also exceeds the GB dislocation spacing $\approx$32 Å, thus

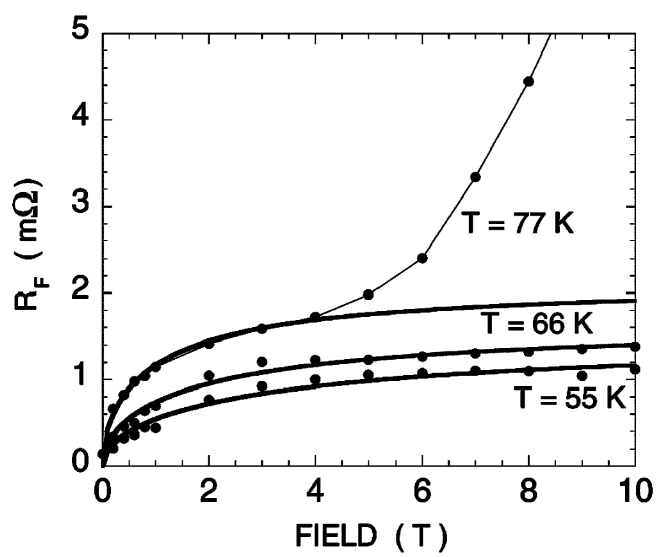

FIG. 4. $R_F(H)$ extracted from the slopes of $V(J)$ for different T and H for the irradiated bicrystal. The V-J curves have the extended linear regions similar to those in Fig. 3. The solid curves are described by Eq. (7).

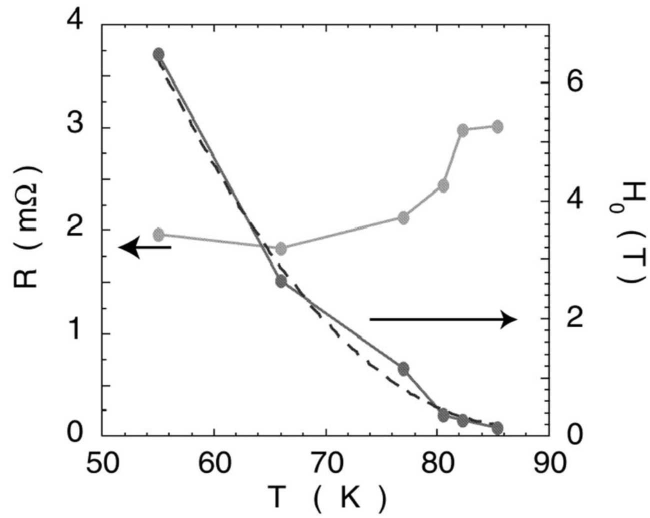

FIG. 5. $R(T)$ and $H_0(T)$ extracted from the fit procedure represented in Fig. 4. The dashed line shows $H_0 = 42(1 - T/T_c)^2$ [Tesla].

the moving AJ cores probe GB properties averaged over few current channels between dislocations. The core length $l(\vartheta) \simeq \xi J_d/J_b(\vartheta)$ increases as ϑ increases, becoming larger than λ, if $\vartheta > \vartheta_0 \ln\kappa$, in which case AJ vortices turn into J vortices. Since the ratio J_b/J_d decreases as T increases, higher-angle GBs can exhibit AJ vortices at low T and J vortices at $T \approx T_c$, while lower angle GBs have A vortices at low T and AJ vortices at $T \approx T_c$.

The depinning current density J_{gb} seen in Fig. 3 is due to interactions of AJ vortices with inhomogeneities along GB and pinned A vortices in the grains [7]. If the periods of AJ and A vortices do not coincide, misfit dislocations in the AJ chain appear. These vortex dislocations can strongly limit J_{gb} [14]. For $H \gg H_{c1}$, the AJ and A periods are close, so the pinning of a few misfit dislocations may be due to macroscopic T_c and $J_b(x)$ variations along GB caused by facet structures, local nonstoichiometry, etc. [16]. In the flux flow state $J \gg J_{gb}$, pinning weakly affects R_F, thus measurements of $R_F(H)$ reveal the physics of GB vortices whose moving AJ cores probe intrinsic properties of GBs at the nanoscale. Because the observed V-J curves are nearly linear above $J_{gb}(77\text{ K}, 1\text{ T}) \sim 10^4$–$10^5$ A/cm$^2 \ll J_b \simeq (0.2$–$0.3)J_d \sim 1 - 10$ MA/cm^2, the region $J \sim J_{gb}$ is much smaller than the scale of Fig. 2. Thus, the nonlinearity of $V(J)$ due to the AJ core expansion does not affect R_F measured at $J < 3J_{gb}$, so Eq. (7) can be used to fit the data. A similar approach was used to measure the flux flow resistivity of pinned A vortices [17].

The case when only a single AJ vortex row moves along the GB, while the intragrain A vortices remain pinned corresponds to low fields, $H < H_1$. For $H > H_1$, the AJ vortices drag neighboring A vortices in the flux flow channel along GB [7]. The field H_1 can be estimated from the condition that the pinning force $f = \phi_0 \Delta H/2a(H)$ of AJ vortices due to their magnetic interaction with A vortices equals the bulk pinning force $\phi_0 J_c/c$, where $\Delta H = \phi_0 e^{-2\pi u/a}/\pi\lambda^2$ is the amplitude of the oscillating part of the local field $H(x) \approx B + \Delta H \cos(2\pi x/a)$ produced by A vortices along GB, and u is the spacing of the first A vortex row from GB. Therefore,

$$H_1 \simeq 4\phi_0 J_c^2(H_1)/c^2 \Delta H^2. \tag{8}$$

The transition from a single to a multiple row vortex motion [9,11] results in a sharp upturn of the $R_F(B, 77\text{ K})$ curve at $H_1 \simeq 4$ T in Fig. 4. Here H_1 for the unirradiated sample ($J_c = 0.1$ MA/cm^2) is 7.3 times smaller than H_1 for the irradiated one ($J_c = 0.27$ MA/cm^2). For $\lambda(77\text{ K}) \simeq 4000$ Å, and $H_1 = 4$ T, Eq. (8) yields $u = \ln(c^2 H_1 \phi_0/4\pi^2\lambda^4 J_c^2)/4\pi = 0.92a$.

In conclusion, vortices on low-angle grain boundaries in HTS are mixed Abrikosov-Josephson vortices. Exact solutions for a moving AJ vortex structure, the nonlinear V-J characteristic and the flux flow resistivity $R_F(B)$ were obtained. From the measurements of $R_F(B)$ on a 7° YBCO bicrystal, we extracted the length of the AJ core and the intrinsic depairing current density J_b on GB. The analysis proposed in this work can be used for systematic studies of the effect of overdoping [4] on current transport through nanoscale channels between GB dislocations.

This work was supported by the NSF MRSEC (DMR 9214707), AFOSR MURI (F49620-01-1-0464), and by Italian INFM-PRA JT3D.

[1] C. C. Tsuei and J. R. Kirtley, Rev. Mod. Phys. **72**, 969 (2000).
[2] H. Hilgenkamp and J. Mannhart (unpublished).
[3] D. C. Larbalestier, A. Gurevich, D. M. Feldmann, and A. A. Polyanskii, Nature (London) **414**, 368 (2001).
[4] S. E. Russek *et al.,* Appl. Phys. Lett. **57**, 1155 (1990); A. Schmehl *et al.,* Europhys. Lett. **47**, 110 (1999); G. Hammerl *et al.,* Nature (London) **407**, 162 (2000); K. Guth *et al.,* Phys. Rev. B **64**, R140508 (2001).
[5] A. Gurevich, Phys. Rev. B **46**, R3187 (1992); **48**, 12 857 (1993); Physica (Amsterdam) **243C**, 191 (1995).
[6] A. Diaz *et al.,* Phys. Rev. Lett. **80**, 3855 (1998); Phys. Rev. B **58**, R2960 (1998).
[7] A. Gurevich and L. D. Cooley, Phys. Rev. B **50**, 13 563 (1994).
[8] D. T. Verebelyi *et al.,* Appl. Phys. Lett. **76**, 1755 (2000); **78**, 2031 (2001).
[9] G. A. Daniels, A. Gurevich, and D. C. Larbalestier, Appl. Phys. Lett. **77**, 3251 (2000).
[10] D. Kim *et al.,* Phys. Rev. B **62**, 12 505 (2000); J. Albrecht *et al.,* Phys. Rev. B **61**, 12 433 (2000).
[11] M. J. Hogg *et al.,* Appl. Phys. Lett. **78**, 1433 (2001).
[12] K. E. Gray *et al.,* Phys. Rev. B **58**, 9543 (1998).
[13] R. D. Redwing *et al.,* Appl. Phys. Lett. **75**, 3171 (1999).
[14] R. Besseling, R. Niggerbrugge, and P. H. Kes, Phys. Rev. Lett. **82**, 3144 (1999).
[15] A. Gurevich and E. A. Pashitskii, Phys. Rev. B **57**, 13 878 (1998).
[16] X. Y. Cai *et al.,* Phys. Rev. B **57**, 10 951 (1998).
[17] M. N. Kunchur *et al.,* Phys. Rev. Lett. **84**, 5204 (2000).